Clinical Imaging 53 (2019) 138–142

Contents lists available at ScienceDirect

Clinical Imaging

journal homepage: www.elsevier.com/locate/clinimag

Cardiothoracic Imaging

Evaluation of pectus excavatum indexes during standard cardiac magnetic resonance: Potential for single preoperative tool☆

Natalia A. Viña[a], Patricia Carrascosa[a], Vanesa C. Mogensen[a], Alejandro Deviggiano[a], Gaston Bellia-Munzon[b], Marcelo Martinez-Ferro[b], Gaston A. Rodriguez-Granillo[a,*]

[a] Department of Computed Tomography and Magnetic Resonance Imaging, Diagnostico Maipu, Buenos Aires, Argentina
[b] Department of Pediatric Surgery, Fundacion Hospitalaria, Private Children's Hospital, Buenos Aires, Argentina

ARTICLE INFO

Keywords:
Chest computed tomography
Nuss procedure: Haller index
Sternum

ABSTRACT

Purpose: Preoperative assessment of patients with pectus excavatum (PE) demands evaluation of malformation indexes, generally with chest computed tomography (CT). In addition, assessment of the cardiac impact of sternal depression has become a rule in high referral centers, thus requiring two independent imaging modalities and use ionizing radiation in a very young population. The objective of this study was to explore the agreement between chest CT and standard cardiac MR (CMR) for the evaluation of chest wall malformation indexes.
Methods: We included consecutive patients with PE referred to undergo chest CT and CMR to establish surgical candidacy and/or to define treatment strategies. Both CT and CMR were performed at full-expiration. In both modalities, the Haller index (HI) and the Correction index (CI) were calculated by two independent observers. In CMR, only scout images were used. Agreement was evaluated using intra-class correlation coefficients (ICC).
Results: Fifty patients comprised the study population (median age 19.0 years) and underwent chest CT and CMR within the same month. CMR assessment of chest malformation indexes was reproducible, with a very good inter-observer agreement for HI [ICC 0.93 (0.88–0.96), $p < 0.0001$] and CI [ICC 0.91 (0.83–0.95), $p < 0.0001$]. CMR also had a very good agreement with chest CT for HI [ICC 0.90 (0.82–0.94), $p < 0.0001$] and CI measurements [ICC 0.93 (95% CI 0.88–0.96), $p < 0.0001$].
Conclusions: We demonstrated an excellent agreement between chest CT and standard CMR for the assessment of chest wall malformations, thus potentially enabling preoperative assessment of PE severity and cardiac involvement with a single diagnostic tool.

1. Introduction

Pectus excavatum (PE) is the most common malformation of the anterior chest wall in children, with male preponderance (male/female ratio 3:2), associated to depression of the sternum and abnormalities of costal cartilages. In general, this chest malformation is present at birth or has an early onset during the first year of life, accentuating during adolescence. Although originally considered an aesthetic condition without clinical implications, several studies conducted in the past decades have demonstrated that PE has a substantial psychosocial impact among developing children [1,2]. Furthermore, it can also can lead to meaningful adverse cardiopulmonary manifestations mainly related to the compression of the right heart side by the depressed chest wall [3,4]. Since the emergence of surgical correction for PE patients with minimally invasive repair, a large number of patients with PE undergo surgery in our clinical environment, requiring preoperative chest computed tomography (CT) in order to evaluate the extent of sternal depression using chest malformation indexes such as the Haller Index (HI) and the Correction index (CI) [4,5]. Importantly, this condition involves a very young population, in whom efforts to avoid ionizing radiation should be maximized [6]. Few previous studies have validated the use of a fast protocol magnetic resonance (MR) as an alternative radiation-free diagnostic tool for the assessment of preoperative malformation indexes [7]. In parallel, cardiac MR (CMR) is a robust technique that can identify the presence and severity of both cardiac morphological and functional abnormalities in patients with PE [8]. Standard CMR imaging involves basic end-expiratory axial scout images with a large field of view that might allow the assessment of chest malformation without the need for additional sequences. Accordingly, with the attempt to achieve a radiation-free one-stop-shop preoperative

☆ None of the authors has conflicts of interest to declare related to the content of the manuscript.

* Corresponding author at: Department of Cardiovascular Imaging, Diagnostico Maipu, Av. Maipú 1668, Vicente López B1602ABQ, Buenos Aires, Argentina.
E-mail address: grodriguezgranillo@gmail.com (G.A. Rodriguez-Granillo).

https://doi.org/10.1016/j.clinimag.2018.10.013
Received 6 June 2018; Received in revised form 10 September 2018; Accepted 12 October 2018

tool for young patients with PE, we sought to explore the agreement between chest CT and CMR for the evaluation of chest wall malformation indexes.

2. Material and methods

2.1. Study population

The present was a retrospective observational study that involved consecutive patients with PE referred to our institution to undergo chest CT and CMR in order to establish surgical candidacy and/or to define treatment strategies. All patients included were older than 8 years old, patients with previous surgical correction of PE, and those who did not provide Habeas data were excluded.

2.2. Chest CT acquisition

Chest CT scans were acquired with a 256-MDCT scanner (ICT, Philips Healthcare) with the following parameters: tube voltage, 80 kVp; tube current, 100 mA; pitch, 0.699; collimation, 128 × 0.625 mm; and rotation time, 0.75 s. Automatic tube current dose modulation (D-DOM, Philips Healthcare) was applied during acquisitions. Images were reconstructed at 1.0-mm-thickness sections. Patients were scanned cranio-caudally during a full-expiration breath-hold.

2.3. Cardiac MR acquisition

CMR examinations were performed with a 1.5 Tesla system (Achieva, Philips Healthcare) using a 5-element cardiac phased-array coil for signal reception and a vector ECG for cardiac synchronization. In our institution, CMR for patients with PE involves a fast protocol (total 20 min appointment) including scout images, steady state free precession (SSFP) cine images in four-chamber, two-chamber, and three-chamber views, as well as a short-axis stack from the mitral valve to the apex. Finally, real-time (free-breathing) cine imaging are acquired in a single mid short-axis and four-chamber views using balanced SSFP sequences in combination with parallel imaging sequences, as previously reported [9]. For the purpose of the present study, only the scout images (standard end-expiratory non-ECG triggered scout fast-field echo images, including axial, coronal, and sagittal views from the supraaortic trunks to the upper renal poles, with unrestricted field of view) were analyzed. Technical parameters of scout images were the following: TR 3.3, TE 1.66 ms, slice thickness 5 mm, matrix 216 × 218, FOV 400 mm, voxel 1.88 × 1.88 mm. This sequence had an approximate duration of 15 s. No specific additional sequences were added to the standard CMR examination. Intravenous contrast material was not administrated for any of the two imaging modalities.

2.4. Chest CT and CMR analysis

Two similarly experienced radiologists blinded to the clinical data performed the analysis of the chest CT indexes and, 60 days later, of the CMR indexes. This lead to different sets of paired comparisons (inter-observer, and inter-method). The site of maximum sternal depression was established using axial and sagittal views, and measurements were performed only in axial views (Fig. 1). In both imaging modalities, two chest wall diameters were measured using axial views at the point of maximal sternal/sternochondral depression: minimum anterior/posterior distance and maximum transverse distance. Using these measurements, the Haller index (HI) was calculated from dividing the transverse distance (the largest horizontal distance of the inside the ribcage) by the minimum anterior/posterior distance (the shortest distance between the anterior spine border and the point of maximal sternal/sternochondral depression). In order to calculate the Correction index (CI), corresponding to the percentage of chest depth to be corrected by the bar placement, an horizontal line was drawn across the anterior spine border and two anterior/posterior distances were measured: the minimum distance between the point of maximal sternal/sternochondral depression and the anterior spine border (Min APd), and the maximum distance between the horizontal virtual line placed on the anterior spine border and the inner margin of the most anterior portion of the chest (Max APd). The CI was therefore calculated as follows: (Max APd − Min APd/Max APd) ∗ 100. Fig. 1 depicts HI and CI calculation with chest CT and CMR. No intravenous contrast was administrated for either imaging modality.

CT effective radiation dose was derived by multiplying the dose-length product with the weighting (k) value of 0.014 mSv/mGy/cm for chest examinations, as suggested by the Society of Cardiovascular Computed Tomography [10].

All procedures performed were in accordance with the ethical standards of the institutional research committee and with the 1964 Helsinki Declaration.

2.5. Statistical analysis

Continuous variables are presented as means ± SD or median (interquartile range), as indicated. The agreement between observers and between imaging modalities were assessed using intra-class correlation coefficients, (ICC; using a two-way random effect model, absolute agreement, and average measurement) with 95% confidence intervals, and also with Bland–Altman plots for continuous variables, consisting of graphs plotting the mean differences and the mean measurements, and enabling determination of the limits of agreement [11]. A two-sided p value of < 0.05 indicated statistical significance. Statistical analyses were performed using SPSS software, version 22 (IBM SPSS Statistics for Windows, Armonk, NY) and MedCalc software (Ostend, Belgium).

3. Results

A total of 50 patients comprised the study population. Forty-two patients (84%) were male, and the median age was 19.0 years (interquartile range 19.0–25.0; minimum 11, maximum 37). All patients underwent chest CT and CMR within the same month. CMR examinations were completed and well tolerated in all cases. The median effective radiation dose of chest CT scans was 1.31 (IQR 1.24; 1.58) mSv, with a median dose-length product of 93.3 (IQR 88.6; 112.5).

A detailed analysis of thoracic measurements performed with chest CT and CMR and discriminated between observers is provided in Table 1. In brief, the mean thoracic indexes of the study population were as follows. Using chest CT, the mean HI was 4.91 ± 1.6 for observer 1, and 4.86 ± 1.6 for observer 2 [ICC 0.98 (95% 0.96–0.99), $p < 0.0001$], and the mean CI was 36.7 ± 15.3% for observer 1 and 31.0 ± 14.2% for observer 2 [ICC 0.90 (95% CI 0.64–0.96), $p < 0.0001$]. Using CMR, the mean HI was 4.93 ± 1.6 for observer 1, and 5.10 ± 1.8 for observer 2 [ICC 0.93 (95% CI 0.88–0.96), $p < 0.0001$], and the mean CI was 34.6 ± 13.8% for observer 1 and 31.3 ± 15.2% for observer 2 [ICC 0.91 (95% CI 0.83–0.95), $p < 0.0001$].

There was a very good agreement between chest CT and CMR regarding the HI measurement both for observer 1 [ICC 0.90 (95% CI 0.82–0.94), $p < 0.0001$] and observer 2 [ICC 0.90 (95% CI 0.82–0.94), $p < 0.0001$]. Similar results were observed for the measurement of the CI, both for observer 1 [ICC 0.93 (95% CI 0.88–0.96), $p < 0.0001$] and observer 2 [ICC 0.95 (95% CI 0.91–0.97), $p < 0.0001$] (Table 2).

Bland-Altman graphs plotting the average differences and the mean measurements for the assessment of inter-observer agreement (Fig. 2), demonstrated near zero mean differences regarding the HI (mean differences between observers: CT 0.02; CMR −0.20); and slightly larger differences for measurements of the CI (mean differences between observers CT 5.7; CMR 3.3). Furthermore, Bland-Altman analysis for the

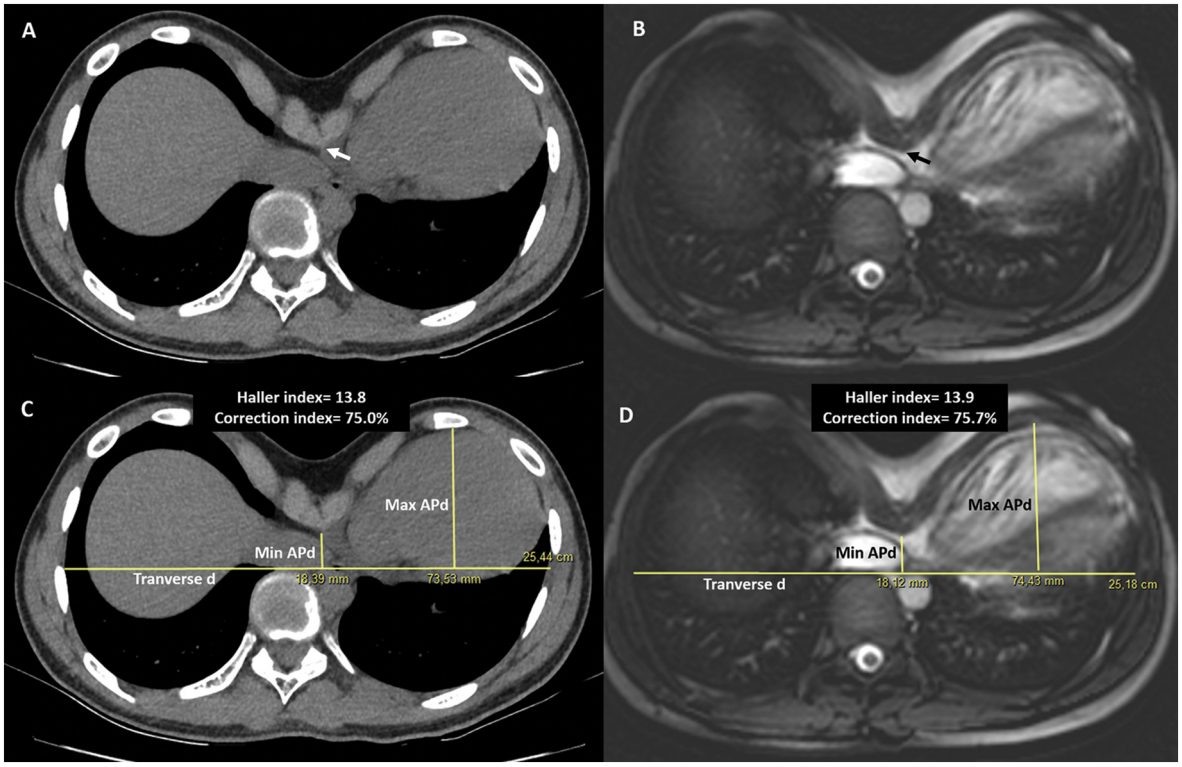

Fig. 1. Measurement of pectus excavatum malformation indexes in a 14-year old male using chest CT (panels A and C) and cardiac magnetic resonance (panels B and D). Axial images at the site of maximum compression (arrows in panels A and B) reveal an excellent agreement between imaging modalities both for Haller and Correction indexes (panels C and D). Min and max APd refer to minimum and maximum anterior/posterior distances, and transverse d refers to transverse diameter.

Table 1
Mean thoracic measurements and indexes.

	Chest CT		Cardiac MR	
	Observer 1	Observer 2	Observer 1	Observer 2
Transverse diameter (mm)	249.6 ± 21.6	243.3 ± 21.5	250.6 ± 20.1	248.2 ± 20.2
Max APd (mm)	88.5 ± 16.3	78.6 ± 14.5	83.9 ± 12.9	77.6 ± 13.5
Min APd (mm)	56.5 ± 19.4	55.0 ± 18.0	55.4 ± 16.8	54.0 ± 17.4
Haller index	4.91 ± 1.6	4.86 ± 1.6	4.93 ± 1.6	5.10 ± 1.8
Correction index (%)	36.7 ± 15.3	31.0 ± 14.2	34.6 ± 13.8	31.3 ± 15.2

Max APd refers to the maximum distance between the horizontal line placed on the anterior spine and the inner margin of the most anterior portion of the chest. Min APd refers to the minimum distance between the posterior sternum and the anterior spine.

assessment of inter-modality agreement showed near zero mean differences regarding the HI (mean differences between modalities: observer 1, 0.0; observer 2, −0.2), and for measurements of the CI (mean differences between modalities: observer 1, 2.1; observer 2, −0.3) (Fig. 3).

4. Discussion

The main finding of our study was the demonstration that images obtained during routine cardiac magnetic resonance (CMR) can provide accurate and reproducible information regarding thoracic malformation indexes among patients with PE, with an excellent agreement with chest CT measurements. Our results might have relevant clinical implications for a number of reasons.

PE patients are typically very young (median 19 years-old in our study), and therefore vulnerable to the risks related to ionizing radiation. Most, if not all, preoperative evaluations of PE involve a chest CT scan to calculate thoracic malformation indexes that enable the determination of the severity of the disease and guide surgical candidacy and strategy [5]. Although the effective radiation dose involved in chest CT scans is generally low (median 1.3 mSv in our study), the youth of PE patients might potentially pose them at a higher risk of developing

Table 2
Inter-observer and inter-modality agreement (intra-class correlation coefficients, ICC).

	Chest CT	Cardiac MR	Observer 1	Observer 2
	Obs 1 vs. obs 2	Obs 1 vs. obs 2	CT vs. CMR	CT vs. CMR
Transverse diameter (ICC, 95% CI)	0.96 (0.59–0.99)	0.98 (0.96–0.99)	0.98 (0.97–0.99)	0.96 (0.86–0.98)
Max APd (ICC, 95% CI)	0.76 (0.23–0.90)	0.76 (0.47–0.88)	0.85 (0.70–0.92)	0.86 (0.76–0.92)
Min APd (ICC, 95% CI)	0.97 (0.95–0.98)	0.98 (0.96–0.99)	0.93 (0.88–0.96)	0.93 (0.88–0.96)
Haller index (ICC, 95% CI)	0.98 (0.96–0.99)	0.93 (0.88–0.96)	0.90 (0.82–0.94)	0.90 (0.82–0.94)
Correction index (ICC, 95% CI)	0.90 (0.64–0.96)	0.91 (0.83–0.95)	0.93 (0.88–0.96)	0.95 (0.91–0.97)

Max APd refers to the maximum distance between the horizontal line placed on the anterior spine and the inner margin of the most anterior portion of the chest. Min APd refers to the minimum distance between the posterior sternum and the anterior spine.

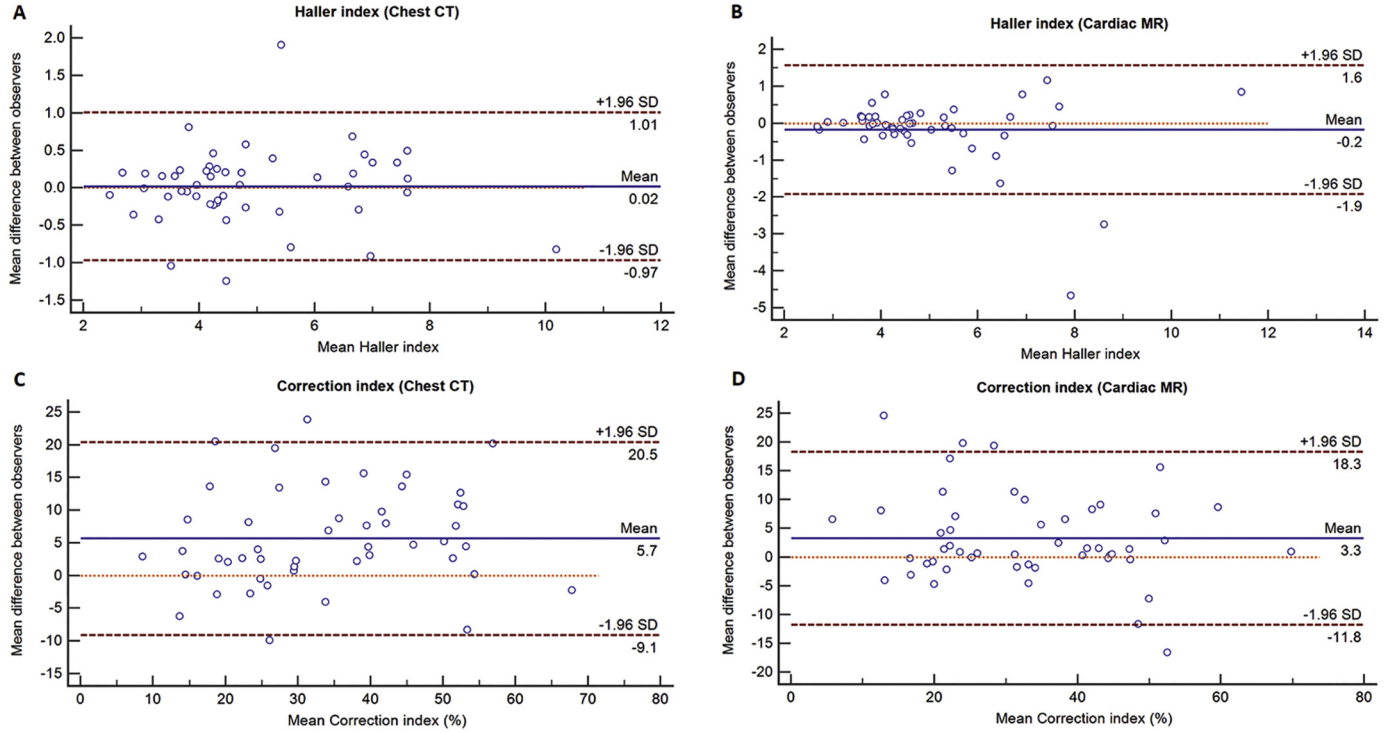

Fig. 2. Inter-observer agreement of Haller (HI, panels A and B) and Correction (CI, panels C and D) indexes discriminated by imaging modality, assessed using Bland-Altman graphs. The graphs illustrate near zero mean differences regarding the HI index and slightly larger differences for measurements of the CI. Note that differences are mildly increased with increasing severity indexes.

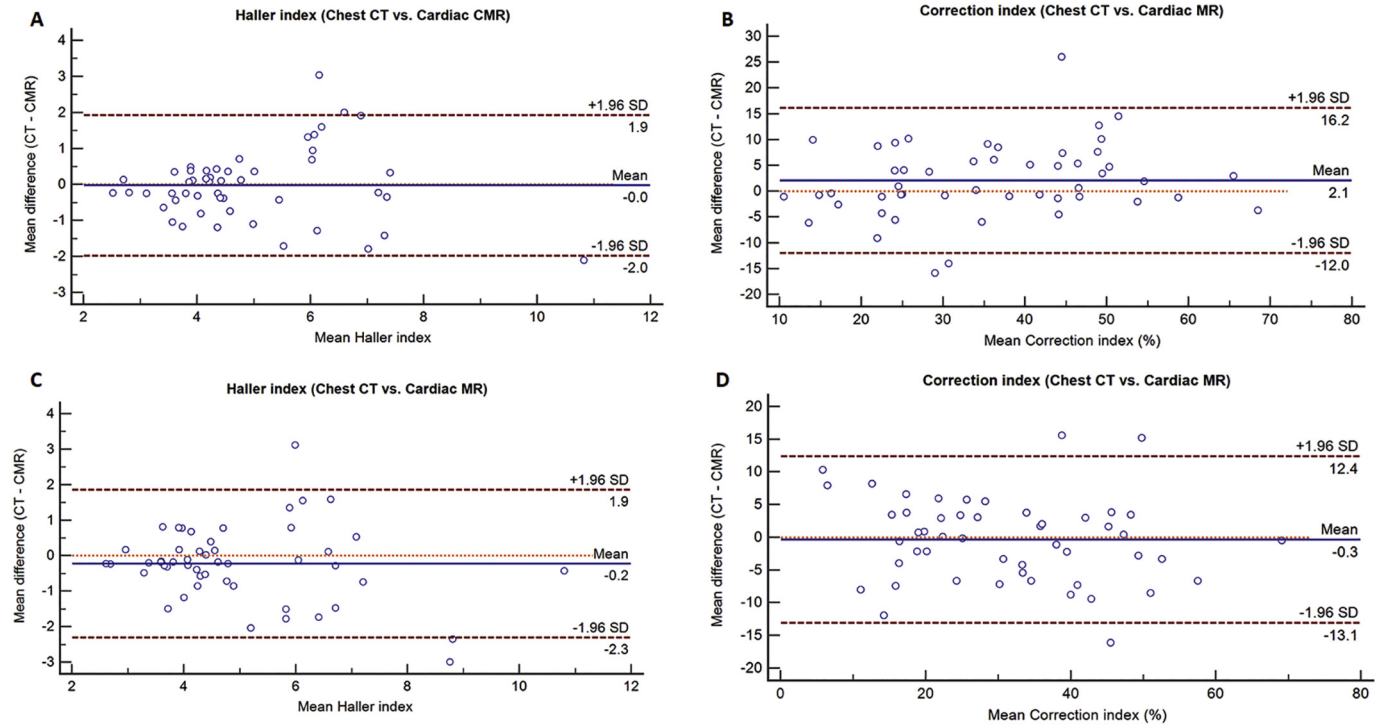

Fig. 3. Inter-modality agreement of Haller (CI) and Correction (CI) indexes discriminated by observer (observer 1, panels A and B; observer 2, panels C and D), assessed using Bland-Altman graphs. The graphs demonstrate near zero mean differences between modalities. Note that HI differences are mildly increased with increasing severity indexes.

radiation-induced malignancies due to the early exposure and to the increased tissue radiosensitivity compared with older patients [12]. In this context, we demonstrated that CMR offers an accurate, reproducible, and radiation-free means to establish PE severity. In contrast to previous investigations that assessed PE severity indexes using chest MR, our is the first study to demonstrate the ability of CMR to provide accurate and reproducible measurements of malformation indexes obtained using a routine CMR protocol, without the need of any

specific additional sequence [7]. Indeed, accurate measurement of PE indexes was achieved using only a scout, non-ECG triggered 15 s sequence. The feasibility of CMR for the evaluation of malformation indexes has been previously reported by Dore et al. and Humphries et al. in very small populations, and their findings were not confronted to chest CT as reference standard [8,13]. Notably, this imaging modality might allow a simultaneous and comprehensive assessment of both the extent and severity of thoracic malformation indexes, as well as of the impact that sternal depression has on cardiac morphology and function [8,9,13]. During the past decade, several studies have shown that compression of the right chambers by the depressed sternum can promote substantial changes in cardiac morphology and function, ranging from none to significant functional impairment [9,14,15]. Consequently, gauging the cardiac impact of PE has become mandatory as part of the preoperative assessment. This can be achieved using both echocardiography and CMR. Although at the expense of higher cost, CMR does not have acoustic window limitations, allows the assessment of cardiac compression during different moments of the respiratory cycle, and provides a better visualization of the right ventricular wall [13,16]. Furthermore, the presence of an exaggerated interventricular dependence, as a reflection of impaired ventricular filling, can be clearly depicted with CMR and has been previously related to the deformation severity [9].

Based on the aforementioned reasons, our study provides proof-of-concept for the potential use of a CMR as a one-stop-shop tool for the preoperative assessment of both thoracic malformation indexes and cardiac impact among patients with PE.

4.1. Limitations

It should be acknowledged that chest CT and CMR measurements were performed by similarly experienced radiologists, in an institution with a high volume of patients with PE. Furthermore, we did not test the ability of experts in cardiac imaging, who are those generally involved in reporting of CMR examinations, to perform thoracic malformation indexes. Accordingly, our results cannot be easily extrapolated to radiology departments with little experience in thoracic malformations.

5. Conclusions

In the present study, we demonstrated the ability of cardiac magnetic resonance to provide accurate data of thoracic malformation indexes in patients with PE using a standard protocol, with an excellent agreement with chest CT measurements. Therefore, CMR might be potentially used as a radiation-free one-stop-shop diagnostic tool for the preoperative assessment of both thoracic malformation indexes and cardiac impact among patients with PE.

References

[1] Lomholt JJ, Jacobsen EB, Thastum M, Pilegaard H. A prospective study on quality of life in youths after pectus excavatum correction. Ann Cardiothorac Surg 2016;5(5):456–65.
[2] Bostanci K, Ozalper MH, Eldem B, Ozyurtkan MO, Issaka A, Ermerak NO, et al. Quality of life of patients who have undergone the minimally invasive repair of pectus carinatum. Eur J Cardiothorac Surg 2013;43(1):122–6.
[3] O'Keefe J, Byrne R, Montgomery M, Harder J, Roberts D, Sigalet DL. Longer term effects of closed repair of pectus excavatum on cardiopulmonary status. J Pediatr Surg 2013;48(5):1049–54.
[4] Abu-Tair T, Turial S, Hess M, Wiethoff CM, Staatz G, Lollert A, et al. Impact of pectus excavatum on cardiopulmonary function. Ann Thorac Surg 2018;105(2):455–60.
[5] Albertal M, Vallejos J, Bellia G, Millan C, Rabinovich F, Buela E, et al. Changes in chest compression indexes with breathing underestimate surgical candidacy in patients with pectus excavatum: a computed tomography pilot study. J Pediatr Surg 2013;48(10):2011–6.
[6] Journy N, Ancelet S, Rehel JL, Mezzarobba M, Aubert B, Laurier D, et al. Predicted cancer risks induced by computed tomography examinations during childhood, by a quantitative risk assessment approach. Radiat Environ Biophys 2014;53(1):39–54.
[7] Lo Piccolo R, Bongini U, Basile M, Savelli S, Morelli C, Cerra C, et al. Chest fast MRI: an imaging alternative on pre-operative evaluation of pectus excavatum. J Pediatr Surg 2012;47(3):485–9.
[8] Humphries CM, Anderson JL, Flores JH, Doty JR. Cardiac magnetic resonance imaging for perioperative evaluation of sternal eversion for pectus excavatum. Eur J Cardiothorac Surg 2013;43(6):1110–3.
[9] Deviggiano A, Vallejos J, Vina N, Martinez-Ferro M, Bellia-Munzon G, Carrascosa P, et al. Exaggerated interventricular dependence among patients with pectus excavatum: combined assessment with cardiac MRI and chest CT. AJR Am J Roentgenol 2017;208(4):854–61.
[10] Halliburton SS, Abbara S, Chen MY, Gentry R, Mahesh M, Raff GL, et al. SCCT guidelines on radiation dose and dose-optimization strategies in cardiovascular CT. J Cardiovasc Comput Tomogr 2011;5(4):198–224.
[11] Bland JM, Altman DG. Agreement between methods of measurement with multiple observations per individual. J Biopharm Stat 2007;17(4):571–82.
[12] Gao Y, Quinn B, Mahmood U, Long D, Erdi Y, St Germain J, et al. A comparison of pediatric and adult CT organ dose estimation methods. BMC Med Imaging 2017;17(1):28.
[13] Dore M, Triana Junco P, Bret M, Gomez Cervantes M, Munoz Romo M, Jimenez Gomez J, et al. Advantages of cardiac magnetic resonance imaging for severe pectus excavatum assessment in children. Eur J Pediatr Surg Feb 2018;28(1):34–8.
[14] Sigalet DL, Montgomery M, Harder J. Cardiopulmonary effects of closed repair of pectus excavatum. J Pediatr Surg 2003;38(3):380–5.
[15] Castellani C, Windhaber J, Schober PH, Hoellwarth ME. Exercise performance testing in patients with pectus excavatum before and after Nuss procedure. Pediatr Surg Int 2010;26(7):659–63.
[16] Lai WW, Gauvreau K, Rivera ES, Saleeb S, Powell AJ, Geva T. Accuracy of guideline recommendations for two-dimensional quantification of the right ventricle by echocardiography. Int J Cardiovasc Imaging 2008;24(7):691–8.